

## Concrete columns reinforced with Zinc Oxide nanoparticles subjected to electric field: buckling analysis

Amir Arbabi, Reza Kolahchi\* and Mahmood Rabani Bidgoli

*Department of Civil Engineering, Jasb Branch, Islamic Azad University, Jasb, Iran*

*(Received January 28, 2017, Revised April 8, 2017, Accepted April 9, 2017)*

**Abstract.** As concrete is most usable material in construction industry it's been required to improve its quality. Nowadays, nanotechnology offers the possibility of great advances in construction. In this study, buckling of horizontal concrete columns reinforced with Zinc Oxide (ZnO) nanoparticles is analyzed. Due to the presence of ZnO nanoparticles which have piezoelectric properties, the structure is subjected to electric field for intelligent control. The Column is located in foundation with vertical springs and shear modulus constants. Sinusoidal shear deformation beam theory (SSDBT) is applied to model the structure mathematically. Micro-electro-mechanic model is utilized for obtaining the equivalent properties of system. Using the nonlinear stress-strain relation, energy method and Hamilton's principal, the motion equations are derived. The buckling load of the column is calculated by Difference quadrature method (DQM). The aim of this study is presenting a mathematical model to obtain the buckling load of structure as well as investigating the effect of nanotechnology and electric field on the buckling behavior of structure. The results indicate that the negative external voltage applied to the structure, increases the stiffness and the buckling load of column. In addition, reinforcing the structure by ZnO nanoparticles, the buckling load of column is increased.

**Keywords:** buckling of concrete column; ZnO nanoparticles; External voltage; difference quadrature method; foundation

### 1. Introduction

A lot of empirical researches have been done for modeling of various structures. These modellings can be divided into two categories of atomic modeling and continuum mechanics (Solhjoo and Vakis 2015). The atomic modeling techniques include: molecular dynamics, molecular dynamics strong bond and theory of Density. This modeling has complex calculations for systems containing many atoms, and also practical applications of this modeling are very limited. On the other hand, with development of continuum mechanics, the limitations of atomic modeling can be overcome. Today continuum mechanics models are widely used for modeling of structures. Comparing atomic and continuum mechanics modeling results show that the continuum mechanics broadly acceptable results in predicting the dynamic and static behavior of systems. So, most researchers to study the dynamic and static behavior of structures used the continuum mechanics.

---

\*Corresponding author, Dr., E-mail: [r.kolahchi@gmail.com](mailto:r.kolahchi@gmail.com)

In recent years, theoretical and experimental studies have been conducted on nano-composites. With the advancement of technology, these structures have opened a special place in the industry and their use is growing. The reason is that using nanoparticles as reinforcement, excellent mechanical and thermal properties can be improved static and dynamic behavior of structures.

Mirza *et al.* (1991) showed that the strength of a short composite steel concrete beam column is affected by variations in the strengths of concrete and steel, the cross sectional dimensions of concrete and steel section, the placement of steel section and reinforcing bars, and the strength model itself. To calculate the properties of composites, Tan and Tong (2001) presented Micro-electromechanical model. Free vibration of composite cylindrical shell containing fluid flow was performed by Kadoli and Ganesan (2003). Wuite and Adali (2005) investigated stress analysis of beams reinforced with carbon nanotubes. They concluded that the presence of carbon nanotubes as reinforcing phase can increase system stability and rigidity. Matsuna (2007) analyzed stability of composite cylindrical shell with the help of third order shear theory. Formica (2010) examined vibrating plate reinforced with carbon nanotubes and for modeling of composite properties, the Mori-Tanaka model was used. Axial failure of RC columns damaged by shear reversals was presented by Henkhaus *et al.* (2013). General information about the definition of slenderness in the well-known standards and ten selected industrial reinforced concrete (RC) chimneys were given by Karaca and Türkeli (2014). Liew *et al.* (2014) studied postbuckling of nano composite cylindrical panels under axial compression. In this study, the mixture law was used to obtain the properties of nanocomposites and meshless method was applied to analyze and calculate the buckling load of nanocomposite structures. The dynamic behavior of composite cylindrical shell containing fluid flow was studied by Seo *et al.* (2015). Stress analysis of cylindrical shells reinforced with carbon nanotubes was presented by Ghorbanpour Arani *et al.* (2015). In this work, asymmetrical thermal load and electric charge as well as magnetic shell were uniform. Buckling analysis of polymeric plates reinforced with carbon nanotubes was studied by Kolahchi *et al.* (2013). They used DQM to obtain structural buckling load. In a work by Kolahchi *et al.* (2016a), dynamic buckling of plates reinforced with functionally graded carbon nanotubes was investigated. Temperature-dependent properties are taken into account and orthotropic Pasternak model is used for simulating the elastic foundation.

In the field of mathematical modeling of concrete structures, Jafarian Arani and Kolahchi (2016) studied buckling of concrete columns reinforced with carbon nanotubes by using Euler - Bernoulli and Timoshenko beam models. Nonlinear buckling of an embedded straight concrete columns reinforced with silicon dioxide (SiO<sub>2</sub>) nanoparticles was investigated by Zamanian *et al.* (2017). According to the scientific search in the database world, there is not any work for investigating the effects of ZnO nanoparticles and electric field on the buckling of the concrete column. So in this work, the smart buckling of concrete columns reinforced with ZnO nanoparticles is presented. In addition, through the presence of ZnO nanoparticles, the structure has piezoelectric properties and is subjected to electric field which is independent of temperature. The micro-electro-mechanical model is used for calculating the equivalent material properties of structure. The concrete column is simulated with SSDT mathematically and DQM is used for obtaining the buckling load of structure. The effects of volume percent of ZnO nanoparticles, external voltage, boundary condition and foundation are shown on the buckling load of system.

### 2. Mathematical modeling

Fig. 1 show a concrete column reinforced with ZnO nanoparticles. The column is located in foundation simulated by vertical spring and shear constants.

In addition, through the presence of ZnO nanoparticles, the structure is subjected to electric filed. Using SSDT, the displacement field can be written as (Thai and Vo 2012)

$$u_1(x, z, t) = u(x, t) - z \frac{\partial w(x, t)}{\partial x} + f\psi(x, t) , \tag{1}$$

$$u_2(x, z, t) = 0 , \tag{2}$$

$$u_3(x, z, t) = w(x, t) , \tag{3}$$

where  $u_1$ ,  $u_2$  and  $u_3$  are the displacement of the mid plane in the axial, transverse and thickness directions;  $\psi$  represents the rotation of cross section about y axis;  $f = \frac{h}{\pi} \sin\left(\frac{\pi z}{h}\right)$ .

Using Eqs. (1) to (3), the nonlinear strain-displacement relations based on Von -Karman theory are as follows

$$\varepsilon_{xx} = \frac{\partial u}{\partial x} - z \frac{\partial^2 w}{\partial x^2} + \frac{1}{2} \left( \frac{\partial w}{\partial x} \right)^2 + f \frac{\partial \psi}{\partial x} , \tag{4}$$

$$\varepsilon_{xz} = \cos\left(\frac{\pi z}{h}\right) \psi . \tag{5}$$

### 3. Piezoelectric materials

When the piezoelectric materials applied to mechanical stress, it creates an electric field in the material. In addition, apply an electric field cause's mechanical strain in the material. In these materials, stress ( $\sigma$ ) and the strain ( $\varepsilon$ ) from the side with an electrical displacement ( $D$ ) and electric field ( $E$ ) from the electrostatic side can be coupled as follows (Ghorbanpour Arani *et al.* 2012)

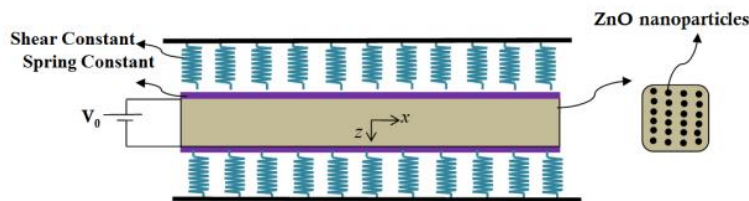


Fig. 1 Schematic of a concrete column reinforced with ZnO nanoparticles

$$\begin{bmatrix} \sigma_{xx} \\ \sigma_{yy} \\ \sigma_{zz} \\ \tau_{yz} \\ \tau_{xz} \\ \tau_{xy} \end{bmatrix} = \begin{bmatrix} Q_{11} & Q_{12} & Q_{13} & 0 & 0 & 0 \\ Q_{12} & Q_{22} & Q_{23} & 0 & 0 & 0 \\ Q_{13} & Q_{23} & Q_{33} & 0 & 0 & 0 \\ 0 & 0 & 0 & Q_{44} & 0 & 0 \\ 0 & 0 & 0 & 0 & Q_{55} & 0 \\ 0 & 0 & 0 & 0 & 0 & Q_{66} \end{bmatrix} \begin{bmatrix} \varepsilon_{xx} \\ \varepsilon_{yy} \\ \varepsilon_{zz} \\ \gamma_{yz} \\ \gamma_{xz} \\ \gamma_{xy} \end{bmatrix} + \begin{bmatrix} 0 & 0 & e_{31} \\ 0 & 0 & e_{32} \\ 0 & 0 & e_{33} \\ 0 & e_{24} & 0 \\ e_{15} & 0 & 0 \\ 0 & 0 & 0 \end{bmatrix} \begin{Bmatrix} E_x \\ E_y \\ E_z \end{Bmatrix}, \tag{6}$$

$$\begin{bmatrix} D_x \\ D_y \\ D_z \end{bmatrix} = \begin{bmatrix} 0 & 0 & 0 & 0 & e_{15} & 0 \\ 0 & 0 & 0 & e_{24} & 0 & 0 \\ e_{31} & e_{32} & e_{33} & 0 & 0 & 0 \end{bmatrix} \begin{bmatrix} \varepsilon_{xx} \\ \varepsilon_{yy} \\ \varepsilon_{zz} \\ \gamma_{yz} \\ \gamma_{xz} \\ \gamma_{xy} \end{bmatrix} + \begin{bmatrix} \varepsilon_{11} & 0 & 0 \\ 0 & \varepsilon_{22} & 0 \\ 0 & 0 & \varepsilon_{33} \end{bmatrix} \begin{Bmatrix} E_x \\ E_y \\ E_z \end{Bmatrix}, \tag{7}$$

where  $Q_{ij}$ ,  $e_{ij}$  and  $\varepsilon_{ij}$  are elastic, piezoelectric and dielectric constants, respectively. The electric field ( $E_k$ ) in terms of electric potential is defined as follows (Ghorbanpour Arani *et al.* 2014)

$$E_k = -\nabla\Phi. \tag{8}$$

In this project, the electric potential distribution is considered as follows

$$\Phi(x, z, t) = -\cos\left(\frac{\pi z}{h}\right)\phi(x, t) + \frac{2V_0 z}{h}, \tag{9}$$

where  $V_0$  is the external voltage. Thus, the electric field in two directions can be obtained as follows

$$E_x = -\frac{\partial\Phi}{\partial x} = \cos\left(\frac{\pi z}{h}\right)\frac{\partial\phi}{\partial x}, \tag{10a}$$

$$E_z = -\frac{\partial\Phi}{\partial z} = -\frac{\pi}{h}\sin\left(\frac{\pi z}{h}\right)\phi - \frac{2V_0}{h}. \tag{10b}$$

According to the SSDT, electromechanical coupling relationship can be summarized as follows

$$\sigma_{xx} = Q_{11}\varepsilon_{xx} + e_{31}\left(\frac{\pi}{h}\sin\left(\frac{\pi z}{h}\right)\phi + \frac{2V_0}{h}\right). \tag{11}$$

$$\sigma_{xz} = Q_{55}\varepsilon_{xz} - e_{15}\left(\cos\left(\frac{\pi z}{h}\right)\frac{\partial\phi}{\partial x}\right), \tag{12}$$

$$D_x = e_{15}\varepsilon_{xz} + \varepsilon_{11}\left(\cos\left(\frac{\pi z}{h}\right)\frac{\partial\phi}{\partial x}\right), \tag{13}$$

$$D_z = e_{31}\epsilon_{xx} - \epsilon_{33} \left( \frac{\pi}{h} \sin \left( \frac{\pi z}{h} \right) \phi + \frac{2V_0}{h} \right), \tag{14}$$

Noted that the using the micro-electro-mechanical model the mechanical and electrical properties of the structure can be obtained by (Tang and Tong 2001)

$$Q_{11} = \frac{C_{11}^r C_{11}^m}{\rho C_{11}^m + (1-\rho) C_{11}^r}, \tag{15a}$$

$$Q_{55} = \frac{1}{\frac{\rho \epsilon_{11}^r}{C_{55}^r \epsilon_{11}^r} + \frac{(1-\rho) \epsilon_{11}^m}{C_{55}^m \epsilon_{11}^m}}, \tag{15b}$$

$$e_{11} = Q_{11} \left[ \frac{\rho e_{11}^r}{C_{11}^r} + \frac{(1-\rho) e_{11}^m}{C_{11}^m} \right], \tag{15c}$$

$$e_{15} = \frac{B}{B^2 + AC} \tag{15d}$$

$$\epsilon_{11} = \frac{C}{B^2 + AC} \tag{15e}$$

$$\epsilon_{33} = \rho \epsilon_{33}^p + (1-\rho) \epsilon_{33}^m - \frac{e_{31}^2}{C_{11}^p} + \frac{\rho (e_{31}^p)^2}{C_{11}^p} + \frac{(1-\rho) (e_{31}^m)^2}{C_{11}^m}, \tag{15f}$$

Where

$$\begin{aligned} A &= \frac{\rho C_{55}^p}{(e_{15}^p)^2 + C_{55}^p \epsilon_{11}^p} + \frac{(1-\rho) C_{55}^m}{(e_{15}^m)^2 + C_{55}^m \epsilon_{11}^m}, \\ B &= \frac{\rho e_{15}^p}{(e_{15}^p)^2 + C_{55}^p \epsilon_{11}^p} + \frac{(1-\rho) e_{15}^m}{(e_{15}^m)^2 + C_{55}^m \epsilon_{11}^m}, \\ C &= \frac{\rho \epsilon_{11}^p}{(e_{15}^p)^2 + C_{55}^p \epsilon_{11}^p} + \frac{(1-\rho) \epsilon_{11}^m}{(e_{15}^m)^2 + C_{55}^m \epsilon_{11}^m}. \end{aligned} \tag{15g}$$

Superscripts *r* and *m* refer to the reinforced and matrix components of the composite, respectively.  $\rho$  also denotes the vol% of the ZnO nanoparticles in the concrete.

#### 4. Governing equations

One of the ways to obtain the governing equations is energy method and the principle of Hamilton. Potential energy of structure taking into account electric field can be written as follows

$$U = \frac{1}{2} \int_V (\sigma_{xx} \varepsilon_{xx} + \sigma_{xz} \varepsilon_{xz} - D_x E_x - D_z E_z) dV, \quad (16)$$

By substituting Eqs. (4) and (5) in Eq. (16), potential energy is as follows

$$U = \frac{1}{2} \int_V \left( \sigma_{xx} \left( \frac{\partial u}{\partial x} - z \frac{\partial^2 w}{\partial x^2} + \frac{1}{2} \left( \frac{\partial w}{\partial x} \right)^2 + f \frac{\partial \psi}{\partial x} \right) + \sigma_{xz} \left( \cos \left( \frac{\pi z}{h} \right) \psi \right) \right. \\ \left. - D_x \left( \cos \left( \frac{\pi z}{h} \right) \frac{\partial \phi}{\partial x} \right) - D_z \left( -\frac{\pi}{h} \sin \left( \frac{\pi z}{h} \right) \phi - \frac{2V_0}{h} \right) \right) dV. \quad (17)$$

The definition of in plane forces and moments are as follows

$$(N, M, P) = \int_A (1, z, f) \sigma_x dA, \quad (18)$$

$$Q = \int_A \cos \left( \frac{\pi z}{h} \right) \sigma_{xz} dA. \quad (19)$$

Using Eqs. (18) and (19), the potential energy can be simplified as follows

$$U = \int_x \left( N \frac{\partial u}{\partial x} + \frac{N}{2} \left( \frac{\partial w}{\partial x} \right)^2 - M \frac{\partial^2 w}{\partial x^2} + P \frac{\partial \psi}{\partial x} + Q \psi \right) dx \\ + \int_V \left( -D_x \left( \cos \left( \frac{\pi z}{h} \right) \frac{\partial \phi}{\partial x} \right) - D_z \left( -\frac{\pi}{h} \sin \left( \frac{\pi z}{h} \right) \phi - \frac{2V_0}{h} \right) \right) dV. \quad (20)$$

The external work due to the foundation around the columns can be expressed as

$$F = -k_w w + k_g \nabla^2 w, \quad (21)$$

In the above equation,  $k_w$  and  $k_g$  respectively are spring and shear constants. However, the external work of the foundation can be written as (Jafarian Arani and Kolahchi 2016)

$$W = \int_x \left( -k_w w + k_g \nabla^2 w \right) w dx. \quad (22)$$

Hamilton's principle is expressed as follows

$$\int_0^t (\delta U - \delta W) dt = 0, \quad (23)$$

Substituting Eqs. (20) and (22) into Eq. (23) yields

$$\delta U = \int_x \left( N \frac{\partial \delta u}{\partial x} + N \frac{\partial \delta w}{\partial x} \frac{\partial w}{\partial x} - M \frac{\partial^2 \delta w}{\partial x^2} + P \frac{\partial \delta \psi}{\partial x} + Q \delta \psi \right) dx \\ + \int_V \left( -D_x \left( \cos \left( \frac{\pi z}{h} \right) \frac{\partial \delta \phi}{\partial x} \right) - D_z \left( -\frac{\pi}{h} \sin \left( \frac{\pi z}{h} \right) \delta \phi \right) \right) dV, \quad (24)$$

$$\delta W = \int_x \left( -k_w w + k_g \nabla^2 w \right) \delta w dx. \tag{25}$$

However, using Hamilton's principal, the four governing equations can be obtained as follows

$$\delta u : \frac{\partial N}{\partial x} = 0, \tag{26}$$

$$\delta w : \frac{\partial^2 M}{\partial x^2} - \frac{\partial}{\partial x} \left( N_x^M \frac{\partial w}{\partial x} \right) - k_w w + k_g \nabla^2 w = 0, \tag{27}$$

$$\delta \psi : \frac{\partial P}{\partial x} - Q = 0, \tag{28}$$

$$\delta \phi : \int_{-h/2}^{h/2} \left( \frac{D_x \pi}{h} \sin \left( \frac{\pi z}{h} \right) + \cos \left( \frac{\pi z}{h} \right) \frac{\partial D_x}{\partial x} \right) dz = 0. \tag{29}$$

By substituting Eqs. (11) and (12) into (18) and (19), the internal forces and moments can be calculated as follows

$$N = hQ_{11} \frac{\partial u}{\partial x} + \frac{hQ_{11}}{2} \left( \frac{\partial w}{\partial x} \right)^2 + 2e_{31}V_0, \tag{30}$$

$$M = -Q_{11}I \frac{\partial^2 w}{\partial x^2} + \frac{24Q_{11}I}{\pi^3} \frac{\partial \psi}{\partial x}, \tag{31}$$

$$P = -\frac{24Q_{11}I}{\pi^3} \frac{\partial^2 w}{\partial x^2} + \frac{6Q_{11}I}{\pi^2} \frac{\partial \psi}{\partial x} + \frac{e_{31}h}{2} \phi, \tag{32}$$

$$Q = \frac{Q_{55}A}{2} \psi - \frac{e_{15}h}{2} \frac{\partial \phi}{\partial x}, \tag{33}$$

where

$$(A, I) = \int_A (1, z^2) dA. \tag{34}$$

Now, inserting Eqs. (30) to (33) in Eqs. (26) to (29), the governing equations can be expressed as

$$\delta u : \frac{\partial^2 u}{\partial x^2} + \frac{\partial w}{\partial x} \frac{\partial^2 w}{\partial x^2} = 0, \tag{35}$$

$$\delta w : -Q_{11}I \frac{\partial^4 w}{\partial x^4} + \frac{24Q_{11}I}{\pi^3} \frac{\partial^3 \psi}{\partial x^3} - \left( 2e_{31}V_0 + N_x^M \right) \frac{\partial^2 w}{\partial x^2} - k_w w + k_g \nabla^2 w = 0, \tag{36}$$

$$\delta\psi: -\frac{24Q_{11}I}{\pi^3} \frac{\partial^3 w}{\partial x^3} + \frac{6Q_{11}I}{\pi^2} \frac{\partial^2 \psi}{\partial x^2} + \frac{e_{31}h}{2} \frac{\partial \phi}{\partial x} - \frac{Q_{55}A}{2} \psi + \frac{e_{15}h}{2} \frac{\partial \phi}{\partial x} = 0, \quad (37)$$

$$\delta\phi: -\frac{2h}{\pi} \frac{\partial^2 w}{\partial x^2} + \frac{h}{2} \frac{\partial \psi}{\partial x} - \frac{\pi^2 \epsilon_{33}}{2h} \phi + \frac{h}{2} \frac{\partial \psi}{\partial x} + \frac{h \epsilon_{11}}{2} \frac{\partial^2 \phi}{\partial x^2} = 0. \quad (38)$$

## 5. DQM

DQM is a numerical method which changes the differential equations to algebraic equations using weighting coefficients. Thus, at any point, derived as a linear sum of the weighted coefficients and values of the function at that point and other points in the direction of the axis will be expressed. The main relationship of DQM, can be expressed as follows (Kolahchi *et al.* 2016b, Kolahchi and Moniribidgoli 2016c)

$$\frac{df}{dx} \Big|_{x=x_i} \rightarrow = \sum_{j=1}^N C_{ij} f_j, \quad (39)$$

So that  $f(x)$  is a function,  $N$  is the number of grid points and  $C_{ij}$  presents weighting coefficients. The roots of the polynomial Chebyshev heavily used in solving engineering problems and bring good results. Of separation is expressed as follows

$$X_i = \frac{L}{2} \left[ 1 - \cos \left( \frac{i-1}{N-1} \pi \right) \right] \quad i = 1, \dots, N. \quad (40)$$

With the roots of polynomial Lagrange transferred as the algebraic relations for calculating the weighting coefficients obtained

$$C_{ij}^{(1)} = \frac{L_1(x_i)}{(x_i - x_j)L_1(x_j)} \quad \text{for } i \neq j, \quad i, j = 1, 2, \dots, N, \quad (41)$$

$$C_{ii}^{(1)} = - \sum_{j=1, j \neq i}^N C_{ij}^{(1)} \quad \text{for } i = j, \quad i = 1, 2, \dots, N, \quad (42)$$

In these two equations

$$L(x_i) = \prod_{\substack{j=1 \\ j \neq i}}^{N_x} (x_i - x_j). \quad (43)$$

And for higher derivative, we have

$$C_{ij}^{(n)} = n \left( C_{ii}^{(n-1)} C_{ij}^{(1)} - \frac{C_{ij}^{(n-1)}}{(x_i - x_j)} \right) \quad i \neq j. \tag{44}$$

Boundary condition equations are

- **Clamped- Clamped (CC)**

$$\begin{aligned} w = u = \phi = \psi = \frac{\partial w}{\partial x} = 0, & \quad @ \quad x = 0 \\ w = u = \phi = \psi = \frac{\partial w}{\partial x} = 0. & \quad @ \quad x = L \end{aligned} \tag{45}$$

- **Clamped- Simple (CS)**

$$\begin{aligned} w = u = \phi = \psi = \frac{\partial w}{\partial x} = 0, & \quad @ \quad x = 0 \\ w = u = \phi = \frac{\partial \psi}{\partial x} = \frac{\partial^2 w}{\partial x^2} = 0. & \quad @ \quad x = L \end{aligned} \tag{46}$$

- **Simple- Simple (SS)**

$$\begin{aligned} w = u = \phi = \frac{\partial \psi}{\partial x} = \frac{\partial^2 w}{\partial x^2} = 0, & \quad @ \quad x = 0 \\ w = u = \phi = \frac{\partial \psi}{\partial x} = \frac{\partial^2 w}{\partial x^2} = 0. & \quad @ \quad x = L \end{aligned} \tag{47}$$

Boundary condition equations due to having weight coefficients, equations are coupled ruling. As a result of the boundary condition and the field should be separated from each other. The governing equations and boundary conditions can be written in matrix form as follows

$$\left( \left[ \underbrace{K_L + K_{NL}}_K \right] + P[K_g] \right) \begin{Bmatrix} \{d_b\} \\ \{d_d\} \end{Bmatrix} = 0, \tag{48}$$

In these relationships,  $P$  is the buckling load. Also,  $[K_L]$ ,  $[K_{NL}]$  and  $[K_g]$  respectively, represents the stiffness matrix linear, nonlinear part of stiffness matrix and geometric matrix . However, using eigenvalue problem, the buckling load of structure can be obtained.

## 6. Numerical results

In this chapter, using the DQM, buckling load of the structure is calculated and the effect of various parameters such as volume percentage of ZnO nanoparticles, geometrical parameters, foundation and external voltage on the buckling load of the column is examined. For this purpose, a concrete column with elastic modulus of  $E_m = 20 \text{ GPa}$  reinforced with ZnO nanoparticles with elastic modulus of  $E_r = 140 \text{ GPa}$  is considered. This chapter consists of three parts examining

the convergence of numerical method, validation and the effects of various parameters on the buckling load of structure. It should be noted that buckling load provided in this section, is dimensionless ( $P = N_x^M / (E_m h)$ ).

### 6.1 Convergence of DQM

Fig. 2 represents the structural buckling load of column versus the number of grid points. As can be seen, with increasing the number of grid points, the buckling load decreases as far as in  $N = 15$ , it is converged. So the calculations in the project are done with 15 grid points.

### 6.2 Validation

Buckling of concrete columns reinforced with ZnO nanoparticles has not been studied by any researcher. So to verify our results, eliminating the effects of zinc oxide nanoparticles ( $\rho = 0$ ), foundations ( $k_w = k_g = 0$ ) and piezoelectric properties, buckling analysis of a beam with SSDT is discussed. Considering the material and the geometric parameters similar to Thai and Vo (2012), buckling load was shown for different aspect ratios of structure in Table 1. As can be observed, the results of the present work in accordance with reference Thai and Vo (2012) show that the results are accurate. It should be noted that the small difference between current results and reference Thai (2012) is due to the difference in type theory. In this project, SSDT is used while in Thai (2012), Timoshenko beam theory is applied.

### 6.3 Buckling analysis

The effect of volume percent of ZnO nanoparticles on the dimensionless buckling load of the structure versus the number of longitudinal mode is shown in Fig. 3. To the point where it is minimal buckling load, is said to be critical buckling load. The critical buckling is reached in third longitudinal mode. Moreover, increasing the volume fraction of nanoparticles increases the buckling load of column. The reason for this is that by increasing the volume fraction of nanoparticles, a higher number of nanoparticles in the columns are glazed and the surface area is reduced. It is also concluded that the effects of ZnO nanoparticles become more remarkable at higher modes.

Table 1 Validation of present work with other published works

$L/h$	TBT, Thai (2012)	SSDBT, Thai and Vo (2012)	SSDT, present
<b>5</b>	8.9509	8.9533	8.9532
<b>10</b>	9.6227	9.6232	9.6231
<b>20</b>	9.8067	9.8068	9.8068
<b>10</b>	9.8671	9.8671	9.8671
<b>0</b>			

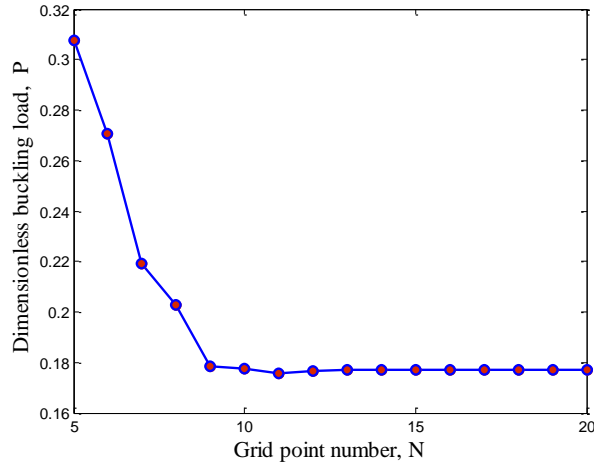


Fig. 2 convergence and accuracy of DQM

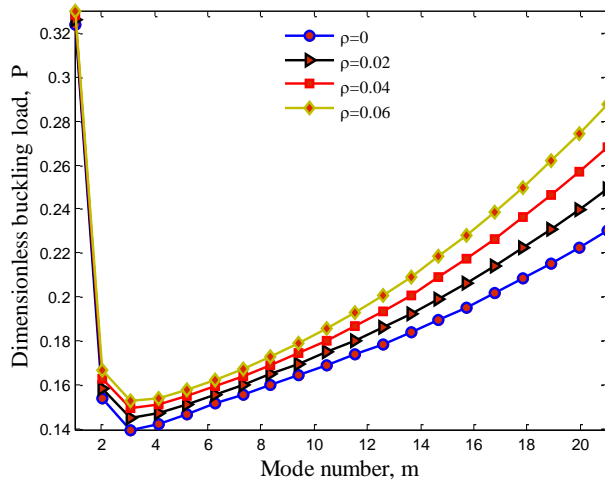


Fig. 3 ZnO volume percent effects on the dimensionless buckling load versus mode number

Fig. 4 shows the dimensionless external applied voltage ( $V^* = V_0 / (h\sqrt{E_r / \epsilon_{11}})$ ) effects on the dimensionless buckling load of columns versus the number of longitudinal mode. As can be seen, an applied negative external voltage causes to compressive force and increasing the buckling load of the system. This phenomenon is converse for positive external voltage. However, it can be concluded that applying external voltage is an effective controlling parameter for buckling behavior of concrete column.

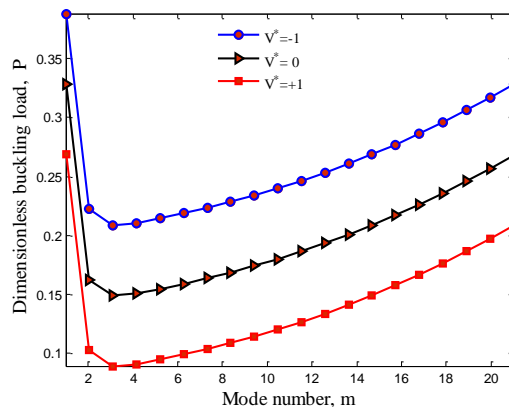


Fig. 4 External electric voltage effects on the dimensionless buckling load versus mode number

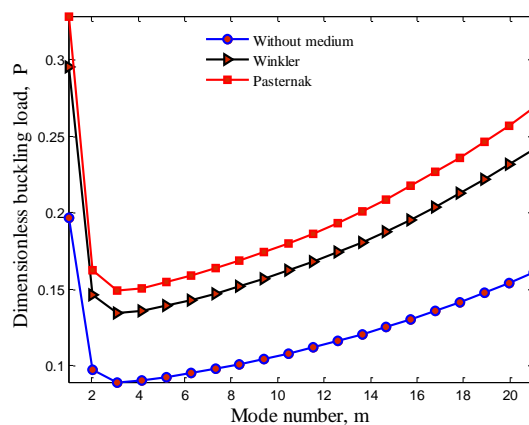


Fig. 5 Foundation effects on the dimensionless buckling load versus mode number

Fig. 5 demonstrates the foundation effect on the dimensionless buckling load based on the number of longitudinal mode. Three types of foundation are considered namely as without foundation, modeling foundation with vertical springs (Winkler) and modeling foundation with vertical springs and shear layer (Pasternak). It can be seen that the buckling load of the column is increased with considering foundation. In addition, the buckling load of the column with Pasternak foundation is more than buckling of the column with Winkler one. The reason for this is that in the model of Pasternak in addition to the flexibility factor, the effect of shear force is also considered.

Fig. 6 illustrates the effect of boundary conditions on the buckling load against the number of longitudinal mode. It can be found that the boundary conditions have a significant effect on the system buckling. In the column with the clamped boundary conditions at both ends, buckling load is maximum with respect to other cases. The reason is that the CC boundary condition yields to maximum stiffness in structure with respect to other cases. In addition, the buckling load of column with fixed-simple boundary condition is higher than Simple-Simple one.

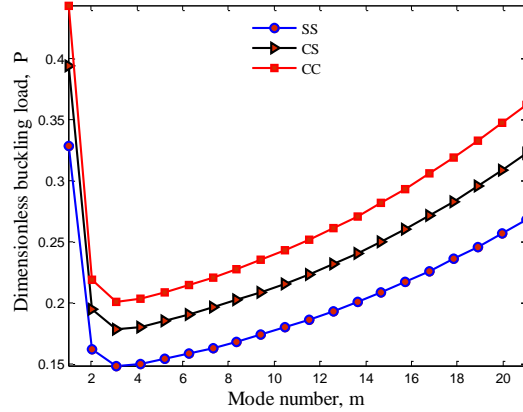


Fig. 6 Boundary condition effects on the dimensionless buckling load versus mode number

Figs. 7-9 present the dimensionless buckling load of structure versus dimensionless external voltage. According to figures, by changing the applied voltage to the structure from negative to positive, buckling load decreases. So applying a negative voltage leads to increase in the structural buckling load while applying a positive voltage has opposite effect, namely to reduce structural buckling load. In other words, a negative voltage leads to more rigidity while the positive voltage causes to softer structure. The reason for this is that the positive and negative voltage cause compressive and tensile force, respectively. Therefore, it can be used to control the buckling load of concrete columns.

The effect of ZnO nanoparticles volume percent on the dimensionless buckling load is shown in Fig. 7. Zero volume percent represents the homogeneous concrete columns. According to the figure, with increasing volume fraction of nanoparticles, due to the increased rigidity of the system, buckling load increases.

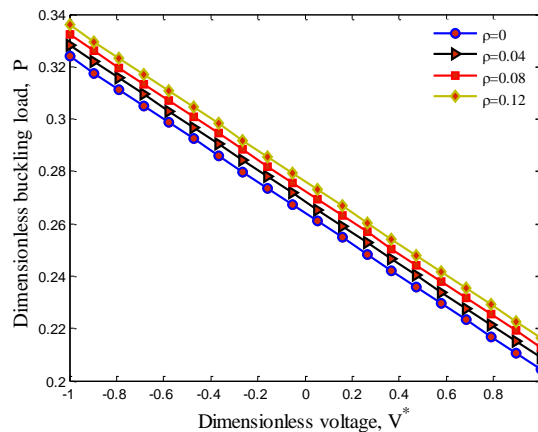


Fig. 7 ZnO volume percent effects on the dimensionless buckling load versus external electric voltage

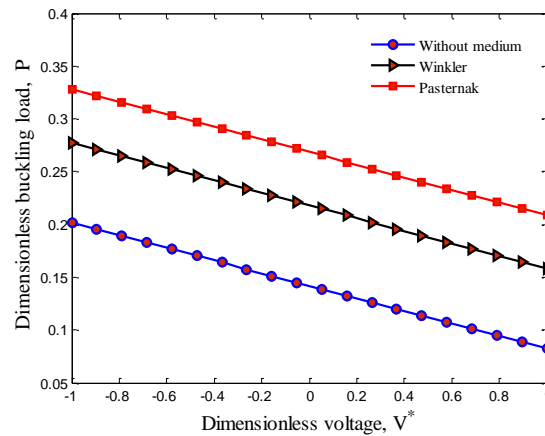


Fig. 8 Foundation effects on the dimensionless buckling load versus external electric voltage

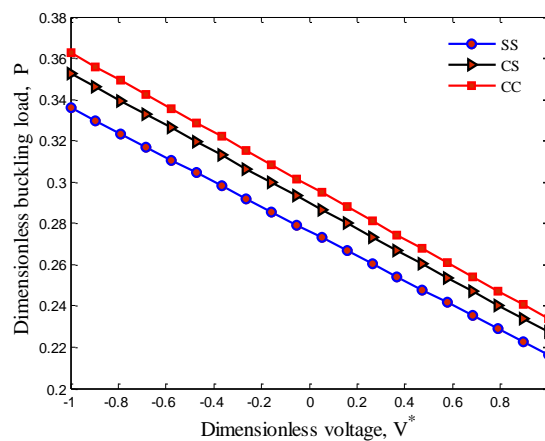


Fig. 9 Boundary condition effects on the dimensionless buckling load versus external electric voltage

In this project, the foundation effect as vertical springs and shear layer is simulated. The effect of foundation on the dimensionless buckling load of the structure is illustrated in Fig. 8. In general foundation increases the buckling load due to the increased rigidity of the system. The buckling load of Pasternak foundation is higher than Winkler one since in the Pasternak foundation, in addition to the vertical loads, shear effects are also considered.

Fig. 9 demonstrates the dimensionless buckling load of structure for different boundary conditions. As can be seen, buckling of the column with the clamped-clamped boundary condition is maximum while the simple-simple boundary conditions for columns has the lowest buckling load between the three modes. The reason for this is that the clamped-clamped boundary condition, the stiffness is maximum and the simple-simple boundary condition, the stiffness is less.

## 7. Conclusions

In this study, buckling of embedded concrete columns reinforced with ZnO nanoparticles subjected to electric field was studied. The foundation was simulated by vertical springs and shear constants. The structure was modeled by SSDT mathematically. Using the strain-displacement equations, energy method and Hamilton's principal, the coupled governing equations was derived. Finally, using DQM, the buckling load of the structure was calculated and the effects of various parameters such as volume percentage of ZnO nanoparticles, external voltage and the foundation were investigated on the buckling behavior of structure. Results indicate that the critical buckling load occurs in approximately third longitudinal mode. With increasing the volume percent of ZnO nanoparticles, the buckling load was increased. In general, existence of foundation increases the buckling load of structure. In addition, the boundary conditions have a significant effect on the column buckling load. The results were validated with other published works. Finally, it is hoped that the results of this work can be useful in concrete structure armed with nanoparticles.

## References

- Formica, G., Lacarbonara, W. and Alessi, R. (2010), "Vibrations of carbon nanotube reinforced composites", *J. Sound Vib.*, **329**(10), 1875-1889.
- Ghorbanpour Arani, A., Kolahchi, R. and Vossough, H. (2012), "Buckling analysis and smart control of SLGS using elastically coupled PVDF nanoplate based on the nonlocal Mindlin plate theory", *Physica B*, **407**(22), 4458-4466.
- Ghorbanpour Arani, A., Fereidoon, A. and Kolahchi, R. (2014), "Nonlinear surface and nonlocal piezoelectricity theories for vibration of embedded single-layer boron nitride sheet using harmonic differential quadrature and differential cubature methods", *J. Intel. Mat. Syst. Str.*, **17**, 1-12.
- Ghorbanpour Arani, A., Haghparast, E., Khoddami Maraghi, Z. and Amir, S. (2015), "Static stress analysis of carbon nano-tube reinforced composite (CNTRC) cylinder under non-axisymmetric thermo-mechanical loads and uniform electro-magnetic fields", *Compos. Part B: Eng.*, **68**, 136-145.
- Henkhaus, K., Pujol, S. and Ramirez, J. (2013), "Axial failure of reinforced concrete columns damaged by shear reversals", *J. Struct. Eng. - ASCE*, **73**, 1172-1180.
- Jafarian Arani, A. and Kolahchi, R. (2016), "Buckling analysis of embedded concrete columns armed with carbon nanotubes", *Comput. Concrete*, **17**(5), 567-578.
- Kadoli, R. and Ganesan, N. (2003), "Free vibration and buckling analysis of composite cylindrical shells conveying hot fluid", *Compos. Struct.*, **60**(1), 19-32.
- Kolahchi, R., Rabani Bidgoli, M., Beygipoor, Gh. and Fakhari, M.H. (2013), "A nonlocal nonlinear analysis for buckling in embedded FG-SWCNT-reinforced microplates subjected to magnetic field", *J. Mech. Sci. Tech.*, **5**, 2342-2355.
- Kolahchi, R., Safari, M. and Esmailpour, M. (2016a), "Dynamic stability analysis of temperature-dependent functionally graded CNT-reinforced visco-plates resting on orthotropic elastomeric medium", *Compos. Struct.*, **150**, 255-265.
- Kolahchi, R., Hosseini, H. and Esmailpour, M. (2016b), "Differential cubature and quadrature-Bolotin methods for dynamic stability of embedded piezoelectric nanoplates based on visco-nonlocal-piezoelectricity theories", *Compos. Struct.*, **157**, 174-186.
- Karaca, Z. and Türkeli, E. (2014), "The slenderness effect on wind response of industrial reinforced concrete chimneys", *Wind Struct.*, **18**(3), 281-294.
- Kolahchi, R. and Moniribidgoli, A.M. (2016c), "Size-dependent sinusoidal beam model for dynamic instability of single-walled carbon nanotubes", *Appl. Math. Mech.*, **37**(2), 265-274.
- Liew, K.M., Lei, Z.X., Yu, J.L. and Zhang, L.W. (2014), "Postbuckling of carbon nanotube-reinforced

- functionally graded cylindrical panels under axial compression using a meshless approach”, *Comput. Method. Appl. M.*, **268**, 1-17.
- Matsuna, H. (2007), “Vibration and buckling of cross-ply laminated composite circular cylindrical shells according to a global higher-order theory”, *Int. J. Mech. Sci.*, **49**(9), 1060-1075.
- Mirza, S. and Skrabek, B. (1991), “Reliability of short composite beam column strength interaction”, *J. Struct. Eng. – ASCE*, **117**(8), 2320-2339.
- Tan, P. and Tong, L. (2001), “Micro-electromechanics models for piezoelectric-fiber-reinforced composite materials”, *Compos. Sci. Tech.*, **61**(5), 759-769.
- Thai, H.T. and Vo, T.P. (2012), “A nonlocal sinusoidal shear deformation beam theory with application to bending, buckling, and vibration of nanobeams”, *Int. J. Eng. Sci.*, **54**, 58-66.
- Thai, H.T. (2012), “A nonlocal beam theory for bending, buckling, and vibration of nanobeams”, *Int. J. Eng. Sci.*, **52**, 56-64.
- Solhjoo, S. and Vakis, A.I. (2015), “Single asperity nanocontacts: Comparison between molecular dynamics simulations and continuum mechanics models”, *Computat. Mat. Sci.*, **99**, 209-220.
- Seo, Y.S., Jeong, W.B., Yoo, W.S. and Jeong, H.K. (2015), “Frequency response analysis of cylindrical shells conveying fluid using finite element method”, *J. Mech. Sci. Tech.*, **19**(2), 625-633.
- Wuite, J. and Adali, S. (2005), “Deflection and stress behaviour of nanocomposite reinforced beams using a multiscale analysis”, *Compos. Struct.*, **71**(3-4), 388-396.
- Zamanian, M., Kolahchi, R. and Rabani Bidgoli, M. (2017), “Agglomeration effects on the buckling behaviour of embedded concrete columns reinforced with SiO<sub>2</sub> nano-particles”, *Wind Struct.*, **24**(1), 43-57.